AGU PUBLICATIONS

Global Biogeochemical Cycles

RESEARCH ARTICLE

10.1002/2015GB005167

Long-term P weathering and recent N deposition control contemporary plant-soil C, N, and P

J. A. C. Davies[1], E. Tipping[2], E. C. Rowe[3], J. F. Boyle[4], E. Graf Pannatier[5], and V. Martinsen[6]

[1]Lancaster Environment Centre, University of Lancaster, Lancaster, UK, [2]Centre for Ecology and Hydrology, Lancaster, UK, [3]Centre for Ecology and Hydrology, Bangor, UK, [4]Department of Geography and Planning, University of Liverpool, Liverpool, UK, [5]Swiss Federal Institute for Forest, Snow and Landscape Research WSL, Birmensdorf, Switzerland, [6]Norges Miljø- Og Biovitenskaplige Universitet, Ås, Norway

Key Points:

- A new C-N-P model is compared with data from 88 natural sites in northern Europe
- Weatherable P is an important long-term control on contemporary soil C and N
- The model predicts large effects of N deposition on ecosystems C and N

Supporting Information:

- Texts S1 and S2, Tables S1–S6, and Figures S1–S5

Correspondence to:
J. A. C. Davies,
j.davies4@lancaster.ac.uk

Citation:
Davies, J. A. C., E. Tipping, E. C. Rowe, J. F. Boyle, E. Graf Pannatier, and V. Martinsen (2016), Long-term P weathering and recent N deposition control contemporary plant-soil C, N, and P, *Global Biogeochem. Cycles*, *30*, 231–249, doi:10.1002/2015GB005167.

Received 10 APR 2015
Accepted 3 JAN 2016
Accepted article online 6 JAN 2016
Published online 20 FEB 2016

Abstract Models are needed to understand how plant-soil nutrient stores and fluxes have responded to the last two centuries of widespread anthropogenic nutrient pollution and predict future change. These models need to integrate across carbon, nitrogen, and phosphorus (C, N, and P) cycles and simulate changes over suitable timescales using available driving data. It is also vital that they are constrainable against observed data to provide confidence in their outputs. To date, no models address all of these requirements. To meet this need, a new model, N14CP, is introduced, which is initially applied to Northern Hemisphere temperate and boreal ecosystems over the Holocene. N14CP is parameterized and tested using 88 northern Europe plot-scale studies, providing the most robust test of such a model to date. The model simulates long-term P weathering, based on the assumption of a starting pool of weatherable P (P_{weath0}, g m^{-2}), which is gradually transformed into organic and sorbed pools. Nitrogen fixation (and consequently primary production) is made dependent on available P. In the absence of knowledge about the spatial variability of P_{weath0}, N14CP produces good average soil and plant variables but cannot simulate variations among sites. Allowing P_{weath0} to vary between sites improves soil C, N, and P results greatly, suggesting that contemporary soil C, N, and P are sensitive to long-term P weathering. Most sites were found to be N limited. Anthropogenic N deposition since 1800 was calculated to have increased plant biomass substantially, in agreement with observations and consequently increased soil carbon pools.

1. Introduction

Over the last 200 years, the flows of carbon (C), nitrogen (N), and phosphorus (P), and many trace elements, have been modified by increasing population density, intensification of agriculture, and emissions from fossil fuel burning. These disturbances are set to continue and become even more widespread with the need to meet global food and energy needs. Understanding changing nutrient cycles in natural environments is important for understanding and managing future C stocks, water quality, and biodiversity. In this study, a new model of C, N, and P cycles, N14CP, is described, tested, and used to explore long-term and large-scale implications of anthropogenic atmospheric N pollution [*Galloway et al.*, 2004; *Sutton et al.*, 2013] in nonagricultural ecosystems.

While the disturbed C cycle has been the main focus of scientific and public attention, the presence of biological actors within the Earth system, with their requirements for C, N, and P, means that the cycling of these elements is tightly coupled. As such, it is problematic to consider one element in isolation. Terrestrial ecosystems that were once effectively closed with respect to nitrogen and phosphorus have become exporters of these nutrients, leading to eutrophication, acidification, loss of biodiversity, and emission of greenhouse gas N_2O [*B Emmett et al.*, 2010; *Galloway et al.*, 2004; *van Vuuren et al.*, 2010; *Vitousek et al.*, 1997].

To understand and manage ecosystem changes at large spatial and temporal scales, quantitative models are needed for exploring and predicting the changes in soil stores of C, N, and P, fluxes of these nutrients to air and water, and ecosystem response. These models must integrate cycles of C, N, and P and be capable of simulating large areas over long periods that reflect current understanding of process timescales, e.g., C residence time in soil is in the centuries/millennia range for the bulk of soil organic matter (SOM) [*Mills et al.*, 2014].

Many models incorporate C and N cycles—at least 250 as analyzed by *Manzoni and Porporato* [2009]. Far fewer models include P cycling. The CENTURY model [*Parton*, 1996] and Community Land Model-carbon, nitrogen, and phosphorus (CLM-CNP) model [*X Yang et al.*, 2014] are exceptions which integrate C, N, and P cycles. However, applications of CENTURY have largely concentrated on C and N, and where P outputs have been compared to data, these have been at the single-site scale [*Parton et al.*, 2005; *Raich et al.*, 2000]. Likewise, the CLM-CNP model, which concentrates on tropical ecosystems, compares results with observations of net primary productivity but not nutrient pools and fluxes. The Terrestrial-Ocean-aTmosphere Ecosystem Model (TOTEM) model also encompasses C, N, and P cycles, but in contrast to CENTURY and CLM-CNP, TOTEM simulates at a lumped global scale [*Mackenzie et al.*, 2002; *Ver et al.*, 1999]. The focus within TOTEM is the global C cycle, and as such testing against N and P data is not explored. More recently, attempts at distributed modeling at the global scale have been made. *Wang et al.* [2010] developed a global representation of C, N, and P cycles to explore the spatial extent of N and P limitation, and *Goll et al.* [2012] have incorporated P cycling into Jena Scheme for Biosphere Atmosphere Coupling in Hamburg (JSBACH). However, calibration and testing against P measurements have been limited in both of these cases. *Wang et al.* [2010] stated that a rigorous calibration of their model was not undertaken due to lack of global scale data, and used only leaf N:P ratio data, global soil %N estimates, and estimates of soil P fractions. Although their model was evaluated against measurements or estimates of biomass, soil C pool and litter production (which are indirectly controlled by P), evaluation directly relating to P was only carried out against P leaching data. *Goll et al.* [2012] used several P cycling parameters from *Wang et al.* [2010] in their extended version of JSBACH and calibrated biochemical mineralization fluxes from estimates of global soil N:P ratios.

If we are to have confidence in the use of large-scale models to address the wider ecosystem effects of disturbed C, N, and P cycles, it is important to constrain and test them using field observations. A new model, N14CP, is proposed, which is simple enough in terms of its level of detail and input requirements to be applied over long timescales and at spatial scales beyond the site scale but also suitable for testing using site-based data. This model builds upon an existing model of C and N cycles, N14C [*Tipping et al.*, 2012b]. The aim is to create a C-N-P model suitable for a broad range of sites that can be driven with readily available climate, deposition, and soil data to allow regional application that is informed by and tested against observed C, N, and P data, rather than a site-specific model that cannot be generalized, or a large-scale model that is unconstrained against data.

Here outcomes from the parameterization and testing of N14CP are reported, using soil C, N, P, radiocarbon, dissolved organic carbon (DOC), dissolved organic nitrogen (DON), and N leaching data for 88 postglacial northern European sites including broadleaf and coniferous forests, shrublands and grasslands, and young ecosystems with comparatively high soil P availability. The parameterized model is then used to explore the role of P in determining ecosystem C and N stores and fluxes, and ecosystem responses to elevated atmospheric N deposition occurring over the last two centuries.

2. Methods

2.1. N14CP—A Long-Term Regional Scale C-N-P Model

The N14C model [*Tipping et al.*, 2012a, 2012b] of C and N cycles was developed to explore the influence of atmospheric N deposition on terrestrial seminatural ecosystems. It provided a general parameterization (made against a set of plot-scale data), which could operate across multiple sites and be driven with readily accessible data such as mean annual temperature, mean annual precipitation, and N deposition. N14C also simulated radiocarbon (^{14}C) dynamics to constrain the turnover rates of the soil organic matter compartments within the model. The current study extends the N14C model with a simple treatment of P cycling, base cation (BC) weathering, and pH to produce the N14CP model.

In the following subsections, a summary of the functionality of N14C is given, and then the extensions that form N14CP are described. Variables and parameters are listed in Tables 1 and 2, and a full model description is provided in the supporting information.

2.1.1. Summary of the N14C Model

The model simulates a number of linked C and N pools representing vegetation biomass, and soil organic matter (SOM) in two layers—a topsoil layer representing the first 15 cm (to make these values comparable with survey data) and a subsoil layer representing everything below this depth. The model runs on a seasonal (3 month) time step. The structure of N14C is depicted in the schematic in Figure 1.

In both N14C and N14CP, four plant functional types (PFTs) are represented: broadleaf, coniferous, herbaceous vegetation, and shrubs. These represent the dominant PFT at a given site. The vegetation biomass comprises coarse woody and fine soft tissue, defined in terms of C:N ratio for each PFT. The C:N ratio of coarse

Table 1. Model State Variable and Output Variable Notation

Variables	Description	Units
	State variables	
C, N, $P_{bio,fine/coarse}$	C, N, and P stored in fine and coarse plant tissues	$g\ m^{-2}$
C, N, P_{lit}	C, N, and P stored in coarse litter	$g\ m^{-2}$
C, N, $P_{SOM,i}$	C, N, and P stored in compartment i (fast/slow/passive) of the SOM	$g\ m^{-2}$
P_{sorb}	Inorganic phosphorus sorbed to soil surfaces	$g\ m^{-2}$
P_{weath}	Weatherable phosphorus within accessible substrate	$g\ m^{-2}$
BC_{weath}	Weatherable BCs within accessible substrate	$g\ m^{-2}$
$P_{fixavail}$	P available for fixation	$g\ m^{-2}$
N,$P_{avail,excess}$	N and P available for plant growth, and excess after growth	$g\ m^{-2}$
	Output variables	
ΔC, N, P_{DO}	Output of dissolved organic C, N, and P from SOM	$g\ m^{-2}\ dt^{-1}$
ΔN, P_{inorg}	Output of dissolved inorganic N and P from SOM	$g\ m^{-2}\ dt^{-1}$
$\Delta P_{sorbed/desorbed}$	Inorganic P sorbed/desorbed from soil surfaces	$g\ m^{-2}\ dt^{-1}$
ΔN_{fix}	N fixation in topsoil	$g\ m^{-2}\ dt^{-1}$
ΔN, $P_{retained}$	N, P remobilized from foliage before litterfall	$g\ m^{-2}\ dt^{1}$
ΔN, $P_{demand,i}$	N, P demand for plant growth for plant species end-member i	$g\ m^{-2}\ dt^{-1}$
NPP_{pot}, NPP_{act}	Potential and actual net primary productivity	$gC\ m^{-2}\ dt^{-1}$
ΔP, BC_{weath}	Phosphorus and base cation weathering flux	$g\ m^{-2}\ dt^{-1}$
ΔN, P_{immob}	Immobilization flux of N and P	$g\ m^{-2}\ dt^{-1}$
	Input variables	
ΔN, P, BC_{dep}	Deposition of N, P, and BCs	$g\ m^{-2}\ dt^{-1}$
T	Mean quarterly temperature	°C
$F_{T>0}$	Fraction of year with temperatures below 0	-

tissue is constant, but that of fine tissue varies depending upon available N, thereby representing either a transition from N-poor to N-rich species or an enrichment of the fine tissues within a single species or the combined effect of both. The variation in fine tissue C:N is implemented using a mix of two end-members with a high and a low C:N. Following Liebig's law of the minimum, net primary productivity (NPP) in N14C depends on a single limiting factor, which may be temperature, precipitation, or available N.

Nitrogen enters the system from two sources: N deposition and N fixation. The N14C model assumes that N fixation is a fixed value based on literature values, which is downregulated by atmospheric additions of N. This downregulation remains a feature within the N14CP, but the fixation is now related to the availability of P, as described in section 2.1.4.

At each quarterly time step, a fraction of the biomass C is converted to litter. Some of the associated N is also converted, while some is retained by the plant for reuse. The coarse litter does not enter the soil organic

Table 2. Parameter Notation Used in Main Text

Notation	Description	Units
f_{DO}	fractional release of DOC, DON, and DOP in decomposition	proportion
$f_{dep,bypass}$	fraction of deposition bypassing the topsoil	proportion
k_{immobN}	rate constant for N uptake by SOM	dt^{-1}
β_{immobP}	proportionality constant between P immobilization rate constant and N immobilization rate constant(s)	-
$[C{:}N]_{im,lower}$	C:N lower limit on immobilization of N into SOM	$g\ g^{-1}$
$[C{:}N]_{im,upper}$	C:N upper limit on immobilization of N into SOM	$g\ g^{-1}$
$[C{:}P]_{im,lower}$	C:P lower limit on immobilization of P into SOM	$g\ g^{-1}$
$[C{:}P]_{im,upper}$	C:P upper limit on immobilization of P into SOM	$g\ g^{-1}$
k_{sorb}	rate constant for sorption of dissolved inorganic P to soil surfaces	dt^{-1}
k_{desorb}	rate constant for desorption of inorganic P from soil surfaces	dt^{-1}
k_{Nfix}	parameter relating N fixation to P availability	$gN\ gP^{-1}\ m^{-2}$
N_{fixmax}	maximum N fixation	$g\ m^{-2}\ dt^{-1}$
$[C{:}P]_{fixlim}$	C:P ratio limit on P extraction from SOM by root exudates	$g\ g^{-1}$
Q_{10}	change in rate with 10 °C increase in temperature	-
K_{acid}, n_{acid}	parameters describing relation of immobilization and decomposition to pH	
k_{Pweath}, $k_{BCweath}$	Weathering rates for phosphorus and base cation pools	dt^{-1}
P_{weath0}	Initial weatherable phosphorus within accessible substrate	$g\ m^{-2}$
BC_{weath0}	Initial weatherable BCs within accessible substrate	$g\ m^{-2}$

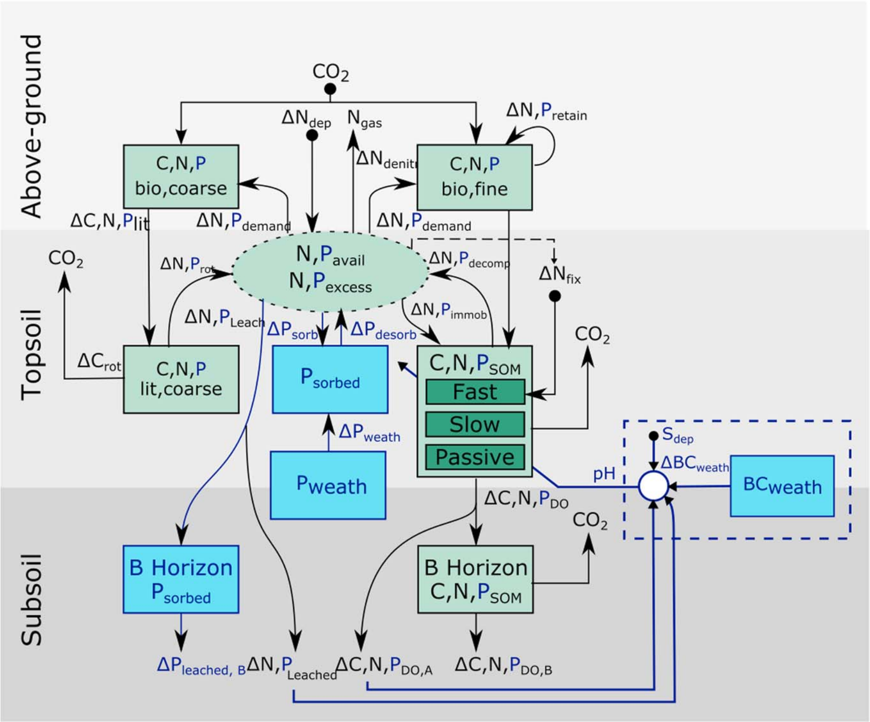

Figure 1. Overview of carbon nitrogen and phosphorus stocks and flows simulated in the N14CP model. New additions in N14CP compared with N14C are highlighted in blue.

matter (SOM) pool but decomposes at the soil surface, contributing N to the soil, but not C. The fine litter contributes to SOM, which is sectioned into three pools, each undergoing first-order decomposition reactions with turnover rates ranging from circa 2 to circa 1000 years following the formulation of *van Veen and Paul* [1981], which is shared by other models such as CENTURY [*Parton*, 1996]. These decomposition rates are modified by a temperature term, where the turnover rates are increased by a factor of Q_{10} for every 10°C increase in temperature

The C loss from decomposition is partitioned into CO_2 and DOC. Nitrogen is lost in proportion to C, consistent with the C:N stoichiometry of each SOM pool, and the N released is partitioned into inorganic N and DON in proportion to the partitioning of released C. The remaining decomposed N is inorganic and, in addition to the inorganic N from deposition, undergoes denitrification according to a temperature-dependent first-order reaction. The residual inorganic N, together with the N retained within the plant prior to litterfall forms the available N for plant growth. If inorganic N remains after plant uptake, immobilization into SOM occurs, and any excess inorganic N is leached.

The SOM in the subsoil layer is fed by organic leachates from the topsoil layer in line with the ideas of [*Kaiser and Kalbitz*, 2012]. The SOM is represented in the subsoil by a single pool with one turnover rate.

2.1.2. N14CP Weathering Inputs of Phosphorus and Base Cations

In N14CP, P, and BCs can enter the plant-soil system by both weathering, i.e., dissolution of parent minerals, and, in principle, atmospheric deposition. Starting pools of weatherable P and BC (P_{weath} and BC_{weath}) are assumed, from which annual releases, ΔP_{weath} and ΔBC_{weath}, are determined by first-order rate constants k_{Pweath} and $k_{BCweath}$, respectively. It is assumed that if the temperature is below 0, then no weathering occurs. This temperature dependency is implemented on an annual basis (like N14C, the majority of the model runs on a seasonal time step, with weathering and pH estimation being exceptions to this) by multiplying the rate constant by the fraction of the year with a mean quarterly temperature above 0 (according to climate input data), $F_{T>0}$. More formally,

$$\Delta P_{weath} = F_{T>0} k_{Pweath} P_{weath} \tag{1}$$

$$\Delta BC_{weath} = F_{T>0} k_{BCweath} BC_{weath} \tag{2}$$

where ΔP_{weath} and ΔBC_{weath} are assumed to enter the topsoil layer of the model and ΔP_{weath} is spread evenly over the quarterly time steps and contributes to an available pool of soil water P, P_{avail}.

The process of weathering here is highly simplified, due to the uncertainties surrounding other factors. Temperature and moisture are known to directly control weathering through their influence on chemical kinetics. The influence of temperature is only crudely incorporated within the model at present since although there is much evidence for temperature effects in laboratory experiments [e.g., *Brady and Carroll*, 1994; *White et al.*, 1999], the influence of temperature in the field is harder to observe and difficult to decouple from other climate-related effects. Inhibition of weathering product release due to saturation of soil water or conversely the reduction of rate limitation due to removal of weathering products by water flow has also been neglected here since the influence of water flow pathways on the contact time between water and rock is highly complex and uncertain. The influence of soil shielding on weathering [*Hartmann et al.*, 2014], i.e., the disconnection of the topsoil from the source material by soil thickness development, is not explicitly included, as this is not a primary issue for the relatively young postglacial soils of northern Europe. However, the first-order approximation of declining P_{weath} and BC_{weath} stock to some degree simulates a disconnecting effect over time. Vegetation and mycorrhizal fungi are recognized to have an influence on weathering processes, through the action of root exudates and nutrient-seeking hyphae [*Berner*, 1992; *Knoll and James*, 1987; *Moulton and Berner*, 1998; *Moulton et al.*, 2000; *Pennington*, 1984; *Quirk et al.*, 2012; *L Taylor et al.*, 2009; *L L Taylor et al.*, 2012; *Volk*, 1987]. However, biota enhanced weathering was omitted here, as the extent to which weathering is controlled by biological activity and the manner in which this should be represented is still under debate.

Whereas P from weathering is intrinsic to the N14CP modeling (see section 2.1.3), the weathering of BCs is only included to allow estimation of the soil water pH, which acts as a control on various soil processes (section 2.1.3). Neither the long-term accumulation of BCs by adsorption to soil solids nor their uptake into plants is simulated.

2.1.3. Soil pH in N14CP

Soil pH is added to the N14CP model and is calculated annually from (1) the atmospheric depositional inputs of sulphate and BCs, (2) weathering inputs of BCs (equation (2)), (3) simulated fluxes of inorganic N (assumed to be nitrate) and DOM, and (4) soil pCO2 (see section S1.5). The pH dependence of soil processes is quantified by a factor α_{pH} given by the following:

$$\alpha_{pH} = \left(1 + \left(\frac{[H^+]}{K_{acid}}\right) n_{acid}\right) - 1 \tag{3}$$

The values of K_{acid} and n_{acid} are defined such that this function allows for a variety of curves where α_{pH} varies between 0 and 1, increasing with pH. This approach is used to modify the decomposition of organic matter and the immobilization of N and P by organic matter (equations (10) and (12)).

2.1.4. Phosphorus Pools

Phosphorus pools are added to the N14C model to form N14CP as illustrated in Figure 1. Biomass P pools are linked to those of C and N, and C:N:P stoichiometries are defined for each PFT. A decomposing coarse litter P pool and soil organic phosphorus (SOP) pool are simulated alongside C and N and are subject to the same turnover rate constants, i.e., the rate constants apply to SOM rather than C, N, and P separately. There is no explicit speciation of organic P, although the three SOM fractions implicitly represent organic P fractions with differing turnovers. The factor α_{pH} is used to modify the decomposition rate

A topsoil pool P_{sorb} represents inorganic phosphorus sorbed to soil mineral surfaces, encompassing both occluded and nonoccluded P. Sorption and desorption of inorganic P from P_{sorb} are determined by the parameters k_{sorb} and k_{desorb}, first-order rate constants that relate P_{sorb} to the dissolved excess inorganic P following growth P_{excess}, i.e.,

$$\Delta P_{sorb} = k_{sorb} P_{excess} \tag{4}$$

$$\Delta P_{desorb} = k_{desorb} P_{sorb} \tag{5}$$

We did not attempt to modify P sorption, because its complex pH dependence (midrange pH minimum) [*Weng et al.*, 2011] precluded extraction of meaningful parameters from field data. A second sorbed P pool, subject to the same dynamics, is simulated in the subsoil layer alongside P in a subsoil SOP pool with one turnover rate.

2.1.5. N14CP Plant Growth

P is included as a limiting factor to plant growth alongside N, temperature, and precipitation within a law-of-the-minimum approach. The potential net primary production ($\mathrm{NPP_{pot}}$) in the model is determined, as in N14C. The actual net primary productivity ($\mathrm{NPP_{act}}$) is then calculated by taking nutrient limitation into account, i.e., the NPP is calculated based on N availability and P availability separately, and then the lower equates to $\mathrm{NPP_{act}}$. P availability for plant growth is defined:

$$\mathrm{P_{avail}} = \Delta \mathrm{P_{retained}} + \Delta \mathrm{P_{decomp}} + \Delta \mathrm{P_{rot}} + \Delta \mathrm{P_{desorb}} + \Delta \mathrm{P_{weath}} + \Delta \mathrm{P_{DO}} + \mathrm{P_{cleave}} \tag{6}$$

where $\Delta \mathrm{P_{retained}}$ is the P that was remobilized and retained within the plant before the previous litterfall, $\Delta \mathrm{P_{decomp}}$ and $\Delta \mathrm{P_{rot}}$ are the inorganic P released from decomposition of the SOM and coarse litter pool, respectively, $\Delta \mathrm{P_{DO}}$ is the dissolved organic P, and $\mathrm{P_{cleave}}$ are the organic forms of P that may be accessible to plants through cleaving of bonds by extracellular phosphatase enzymes [*McGill and Cole*, 1981; *Olander and Vitousek*, 2000; *Rowe et al.*, 2008]. To ensure that including this source does not deplete the SOM reservoir unrealistically (i.e., beyond the range of soil N:P observations), the P which may be cleaved from the SOM is assumed to be limited by a maximum C to P ratio, $[\mathrm{C:P}]_{\mathrm{fixlim}}$ as follows:

$$\mathrm{P_{cleave}} = \mathrm{P_{SOM}} - \frac{\mathrm{C_{SOM}}}{[\mathrm{C:P}]_{\mathrm{fixlim}}} \tag{7}$$

The sources of P to plant growth in equation (5) are used preferentially in their order of listing, i.e., P retained within the plant is used first, then readily available inorganic P in soil water is used ($\Delta \mathrm{P_{decomp}} + \Delta \mathrm{P_{rot}} + \Delta \mathrm{P_{desorb}} + \Delta \mathrm{P_{weath}}$), followed by less accessible organic forms $\Delta \mathrm{P_{DO}}$ and $\mathrm{P_{cleave}}$ from the SOM only where the P requirement indicated by the potential NPP exceeds the retained and inorganic sources.

2.1.6. Phosphorus-Dependent Nitrogen Fixation

It is widely assumed that N fixation is to some extent controlled by P availability [*Cleveland et al.*, 1999; *Crews et al.*, 2000; *Eisele et al.*, 1989; *Vitousek et al.*, 2010], and to reflect this a simple functional relationship between N fixation and P availability is included in N14CP. Attempting to explicitly represent the specific availability of P to particular N fixing organisms over time and space would be overly detailed in comparison to other process representation in the model. As such, a simple relationship between the overall amount of P in plant/microbe available forms and N fixation is made, minimizing the additional number of parameters needed. The overall amount of P in plant/microbe available forms $\mathrm{P_{fixavail}}$ is defined equal to $\mathrm{P_{avail}}$ (equation (5)), minus the plant retained P, which is used only for plant growth. N fixation is then assumed to take the following form:

$$\Delta \mathrm{N_{fix}} = \mathrm{N_{fixmax}} \frac{k_{\mathrm{Nfix}} \mathrm{P_{fixavail}}}{k_{\mathrm{Nfix}} \mathrm{P_{fixavail}} + 1} - \Delta \mathrm{N_{dep}} \left(1 - f_{\mathrm{dep,bypass}}\right) \tag{8}$$

where $\mathrm{N_{fixmax}}$ is a temperature-dependent value determining the maximum fixation, k_{Nfix} is a constant controlling the degree to which P availability limits fixation, and $f_{\mathrm{dep,bypass}}$ controls the fraction of deposition that makes sustained contact with the topsoil.

Adding this dependency of N fixation on P availability means that while a law-of-the-minimum approach is taken to calculating NPP, colimitation can develop in the modeled system as advocated by *Danger et al.* [2008], through P limitation of N fixation.

2.1.7. Immobilization Processes

In the N14C model [*Tipping et al.*, 2012a, 2012b], if there was an excess of N after growth ($\Delta \mathrm{N_{excess}}$), then this would be available for immobilization into the SOM such that

$$\Delta \mathrm{N_{immob}} = k_{\mathrm{immobN}} \Delta \mathrm{N_{excess}} \mathrm{C_{SOM}} Q_{10}^{T/10} \tag{9}$$

where k_{immobN} is the immobilization factor. This has been extended here to include a pH effect and stoichiometric effect such that

$$\Delta \mathrm{N_{immob}} = k_{\mathrm{immobN}} \Delta \mathrm{N_{excess}} \mathrm{C_{SOM}} Q_{10}^{T/10} \alpha_{\mathrm{pH}} \alpha_{\mathrm{C:N}} \tag{10}$$

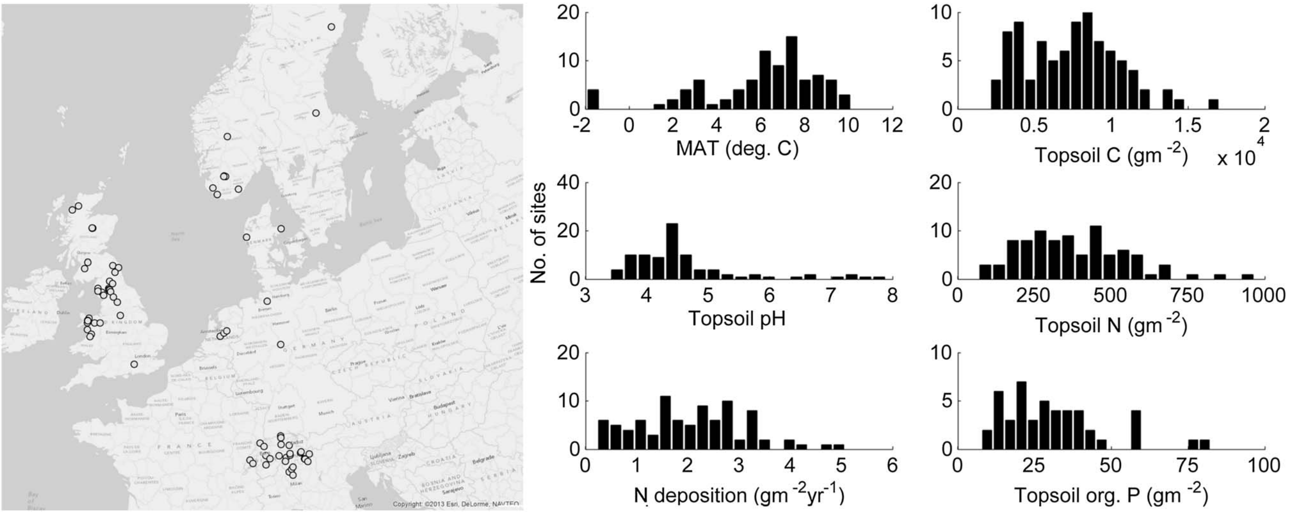

Figure 2. Site data locations and distributions of mean annual temperature (MAT), soil pH, nitrogen deposition in year 2000, and observed organic topsoil carbon, nitrogen, and phosphorus contents. Data are detailed in the SI, Tables S3–S5 [*Andersson et al.*, 2002; *Beier et al.*, 2009; *Berggren et al.*, 2004; *Blaser et al.*, 2005; *Bloemerts and Vries*, 2009; *Corre and Lamersdorf*, 2004; *de Vries et al.*, 2005; *UKREATE*, 2010; *DEFRA*, 2006; *B A Emmett et al.*, 2004; *Evans et al.*, 2005; *Gundersen*, 1995; *Jackson-Blake et al.*, 2012; *Kleja et al.*, 2008; *Kreutzer et al.*, 1998; *Lamersdorf and Meyer*, 1993; *MacDonald et al.*, 2002; *Mol-Dijkstra and Kros*, 1999; *Parr et al.*, 1998; *Pilkington et al.*, 2005; *I K Schmidt et al.*, 2004; *Sjøeng et al.*, 2007; *J D Speed et al.*, 2014; *J D M Speed et al.*, 2015; *Tietema et al.*, 1992; *Tipping et al.*, 2008; *van Meeteren et al.*, 2008; *von Oheimb et al.*, 2008; *Walthert et al.*, 2004; *Wright et al.*, 1998; *Zimmermann et al.*, 2006].

where α_{pH} is a scalar that varies with pH as defined in equation (12), and $\alpha_{C:N}$ is a scalar that varies with current SOM C:N such that $\alpha_{C:N}$ is 0 below a C:N threshold $[C:N]_{im,lower}$, 1 above a C:N threshold $[C:N]_{im,upper}$ and a linear approximation between these thresholds:

$$\alpha_{C:N} = \left(\frac{\frac{C_{SOM}}{N_{SOM}} - [C:N]_{im,lower}}{[C:N]_{im,upper} - [C:N]_{im,lower}} \right) \tag{11}$$

where

$$[C:N]_{im,lower} < \frac{C_{SOM}}{N_{SOM}} < [C:N]_{im,upper}$$

A proportionality constant $\beta_{immobP:N}$ is combined with the N immobilization constant so that P immobilization is defined:

$$\Delta P_{immob} = \beta_{immobP:N} k_{immobN} \Delta P_{excess} C_{SOM} Q_{10}^{T/10} \alpha_{pH} \alpha_{C:P} \tag{12}$$

where $\alpha_{C:P}$ takes the same form as $\alpha_{C:N}$ (equation (11)), but using C:P thresholds. Using a multiplier in this way relates the P immobilization rate constant to the N immobilization rate constant for each PFT using only one parameter.

2.1.8. Phosphorus Losses

Phosphorus is lost from the topsoil by the leaching of any P_{inorg} that remains after plant uptake, immobilization, and sorption. A fraction of this excess P_{inorg} enters the subsoil (Figure 1), where further sorption and desorption processes take place as in equation (4). Desorbed subsoil P_{inorg} is subsequently leached. Phosphorus is also lost from the topsoil in DOP, proportioned to DOC by the C:P stoichiometry of the SOM pools. As with DOC, some of the DOP accumulates in the subsoil.

2.2. Data for Model Parameterization and Testing

Field site data comprising soil organic C, N, and P pools, pH, and dissolved organic and inorganic element fluxes were compiled to calibrate and test the N14CP model (Tables S3–S5 in the supporting information). Measurements from broadleaf, coniferous, shrub, and herbaceous seminatural habitats were collated for 88 sites within northern Europe (Figure 2). Care was taken to create a data set with equal numbers of the four PFTs and encompassing a range of temperatures and soil pH. All sites have soil organic C and N measurements and soil pH, while 34 of the sites also have soil organic P data. The data set was then split into two sets of 44 sites: one for model calibration and one for model testing. Again, care was taken to ensure that the two sets had balanced numbers of PFTs and were representative of the range of climate and soil conditions. All the data pertain to the topsoil (0–15 cm), so topsoils are focused on in the model analysis and results.

All sites were simulated from 10,000 B.C., which is roughly the end of the last glaciation for northern Europe. It is assumed that at this time there was neither soil nor plant cover. Site conditions, including contemporary mean annual temperature (MAT), mean annual precipitation (MAP), N, sulfur (S), and BC deposition, were compiled for each site. Site MAT was temporally varied using an anomaly based on *Davis et al.* [2003]. MAP was kept constant over the whole time period due to a lack of information on historical trends. Atmospheric deposition of N and S before 1800 was assumed to be 0, i.e., pristine conditions without anthropogenic inputs were assumed. While there were external inputs of N from lightning during this period, we estimate the magnitude of these to be in the region of 0.003–0.015 $g\,m^{-2}\,a^{-1}$ based on *Shepon et al.* [2007] and *Schumann and Huntrieser* [2007]. These are small compared with rates of N fixation and so are neglected. Other natural sources of N, such as fires and soil NOx, were ignored, as these were not net exogenous inputs of N. Post 1800, the N, and S deposition (ΔN_{dep} and ΔS_{dep}) were assumed to follow the temporal anomaly suggested by *Schöpp et al.* [2003] and BC deposition (ΔBC_{dep}) followed a trend based on *Majer et al.* [2003]. These temporal trends were scaled to match contemporary observations available for each site modeled (Table S4 in the SI). Scavenging due to tree cover is included in the local measurements. Atmospheric P deposition was neglected, as *Tipping et al.* [2014] have shown that there is no systematic variation of P deposition across Europe, and local redistribution of P determines local gains and losses [*Tipping et al.*, 2014]. There is a net input of P to northern Europe from dust sources such as the Sahara [*Mahowald et al.*, 2008]. However, this input is small in comparison to weathering inputs, and given the uncertainty that surrounds further assumptions which would need to be made regarding historical changes in dust sources over the Holocene, this source was assumed to be negligible.

A number of land use histories were defined for different geographical locations and land use types based on the characteristic timings of succession from herbaceous to wooded plant types following deglaciation (that is if succession occurred at all) and woodland clearance dates. These are detailed within the SI, Table S5.

Representative radiocarbon contents of topsoils were assigned on the basis of vegetation cover; forested sites have been shown to have significantly higher radiocarbon values, i.e., greater contents of recently fixed C than those of nonforested soils [*Bol et al.*, 1999; *Mills et al.*, 2014; *Tipping et al.*, 2010; *Tipping et al.*, 2012a, 2012b]. Following *Mills et al.* [2014], we assumed mean $SO^{14}C$ of 111.7 and107.9% modern for forest soils in 1971 and 2004, respectively. For nonforested soils, a mean $SO^{14}C$ of 99.1% modern for 2006 was assumed, and for all sites a $DO^{14}C$ value of 109% modern for 2006 was adopted.

In the absence of measured values, a representative DOC:DOP ratio of 870 $g\,g^{-1}$ was adopted, based on literature values [*Kaiser et al.*, 2003; *Lottig et al.*, 2012; *McGroddy et al.*, 2008; *Qualls and Haines*, 1991; *Yanai*, 1992]. The contemporary inorganic P leaching (ΔP_{inorg}) "target" for parameterization was taken to be 0, but this does not mean that inorganic P leaching is prevented rather that the present-day flux is constrained to be small.

PFT properties including the ratio of coarse to fine plant tissues, the stoichiometric C, N, and P contents of these tissues, and parameters determining litterfall characteristics were set, as shown in Table S6 based on the sources detailed in the SI.

2.3. Model Parameter Sensitivity

Where possible, parameters were set based on literature values, and parameters for processes shared by N14C and N14CP were assigned in keeping with *Tipping et al.* [2012a, 2012b] (Table S2). The weathering rates k_{Pweath} and $k_{BCweath}$ were set in accordance with *Boyle et al.* [2013] to 2.5×10^{-4} and 6.3×10^{-5}, respectively, based on an analysis of lake sediment records and soil chronosequences. The initial base cation pool, BC_{weath0}, was estimated from contemporary pH measurements. The present-day flux of BCs needed to provide the correct pH was calculated, utilizing site or mean levels of DOC and inorganic N leaching and the site-based N and S deposition. This flux was then used to determine the weathering pool needed at this date. A back calculation was then made to project this pool back to the initial condition, based on the known historical temperature.

There remain 10 parameters associated with the new process representations to be defined: $\beta_{\mathrm{immobP:N}}$, f_{DO}, K_{acid}, N_{acid}, k_{Psorb}, k_{Pdesorb}, k_{Nfix}, $[C:P]_{\mathrm{lower}}$, $[C:P]_{\mathrm{high-low}}$, and $[P:C]_{\mathrm{lim}}$. In addition, a parameter was required to characterize the variation of P_{weath0}. As will be explained in section 3, after exploring the use of a constant value for P_{weath0} and attempting to relate P_{weath0} to lithological and soil data for the different sites, the best approach we could find for parameterizing the present data set was to distinguish two sets of soils, podzols and rankers on the one hand, and all remaining soil types on the other. The adjustable parameter then was P_{weath0} for podzols and rankers, with a constant multiplier used to obtain P_{weath0} for the other soils.

We performed a sensitivity analysis to establish which of the 11 parameters have the most influence on the outputs of the model that can be compared against the observations, thus indicating which parameters are most worth exploring and which are insensitive and can be set. The elementary effects method [*Campolongo et al.*, 2007], which considers parameter interactions, was used within the sensitivity analysis. The methodology, applications, and results are described further in the SI (section S2). Overall, the most influential parameters on the outputs are, in order of sensitivity, are as follows: the fraction of adsorption of P onto mineral surfaces (k_{Psorb}); the factor which controls the fraction of C, N, and P from decomposition which is lost in a dissolved organic form (f_{DO}); the initial pool of weatherable P (P_{weath0}); and the parameter relating N fixation to available P (k_{Nfix}). The least influential parameters are $[C:P]_{\mathrm{lower}}$, $[C:P]_{\mathrm{high-low}}$, and $[P:C]_{\mathrm{lim}}$.

As a result of this analysis, k_{Psorb}, f_{DO}, P_{weath0}, k_{Nfix}, $\beta_{\mathrm{immobP:N}}$, K_{acid}, and N_{acid} were explored within the parameterization, and $[C:P]_{\mathrm{lower}}$, $[C:P]_{\mathrm{high-low}}$, and $[P:C]_{\mathrm{lim}}$ were fixed a priori. Although k_{Pdesorb} was shown to have little influence on the majority of observable outputs, it was also explored within the parameterization, as it is the most sensitive parameter in determining the inorganic P leaching flux, and it is coupled closely to k_{Psorb}.

2.4. Model Parameterization and Testing

Half of the sites contained within the data set described in section 2.2 were used for parameterization, leaving half for blind testing. For the parameterization sites a cost function to assess the performance of the parameter set was constructed using observations of SOC, SON, SOP pools, soil C:N and N:P, DOC, DON, and inorganic N leaching. In addition, non-site-specific values of NPP, $SO^{14}C$, $DO^{14}C$, DOC:DOP, and $\Delta P_{\mathrm{inorg}}$ (as described in section 2.2) were also used within this function. Multiple local searches were used to set well-constrained parameters, and a global search used to set less well-constrained parameters. Further details of the methodology are given in SI, section S2.2. The general parameter set obtained by this procedure was subsequently tested against data from the remaining 44 sites.

A second parameterization exercise was undertaken where P_{weath0} was varied on a site-by-site basis for all the sites within the data set, while all other parameters were kept at their generalized values. For each site, P_{weath0} was systematically varied between 50 and 1000 g m^{-2}, since these values gave initial and contemporary P weathering rates in the range 0.75 to 150 kg km^{-2} a^{-1}, covering the range of values (1.5 to 85 kg km^{-2} a^{-1}) estimated by *Hartmann et al.* [2014]. The site-specific observations of SOC, SON, SOP pools, soil C:N, DOC, DON, and inorganic N leaching were then used within a cost function to calibrate P_{weath0} for each site (S2.3 details this further).

3. Results

3.1. N14CP Model Parameterization and Testing

Preliminary trials with N14CP showed that the simulated contemporary soil organic P pool (P_{SOM}), depended strongly upon the value of P_{weath0}, as must be expected for soils of similar age assumed to have undergone the same development processes with respect to the different P pools. Therefore, we sought a predictor of P_{weath0} correlated to the measured P_{SOM}, which ranged from 10 to 80 g m^{-2}. We explored the use of globally mapped lithological data [*Hartmann and Moosdorf*, 2011, 2012; *Hartmann et al.*, 2012, 2014; *Xiaojuan Yang et al.*, 2013], but no correlation with P_{SOM} was found using either rock P concentration or P weathering rate ($r^2 = 0.0$, $n = 47$ in both cases). Then, we considered soil types and found that the average P_{SOM} for the podzols and rankers with measured P_{SOM} ($n = 21$) was significantly lower ($p < 0.02$), by a factor of 1.7 than the average for other soil types ($n = 26$). We used this finding in the general modeling to distinguish P_{weath0} among sites, parameterizing the value for podzols.

Table 3. Model Parameter Values Set Within the Generalized Parameterization[a]

Parameter	Range From 50 Local Searches (Boundaries)	Parameter Set Through Multiple Local Searches	Parameter Set by Reduced Global Search
f_{DO}	0.03–0.032 [0.001, 0.1]	0.0308	-
P_{weath0}	100–149 [100, 1000]	120	-
k_{Nfix}	0.025–0.040 [0.02, 0.2]	0.0286	-
f_{Psorb}	0.94–0.99 [0.8, 0.99]	0.97	-
$k_{immobP:N}$	4.29–19.88 [0.1, 10]	-	8.58
$f_{Pdesorb}$	0.005–0.049 [0.01, 0.05]	-	0.005
K_{acid}	0.024–0.485[1e–6, 0.5]	-	0.364
n_{acid}	0.38–1 [0.1, 1]	-	0.590

[a] The second column from the left gives the range of parameter values found from a set of 50 localized searches and the search boundaries (in square brackets). Following these searches, the first four parameters were found to be well constrained and set as shown in the third column from the left. A globalized search was then performed on the remaining four parameters, resulting in parameter values as shown in the last column.

The general parameter set is given in Table 3, and model results are plotted against observations for the 44 parameterization and 44 testing sites in Figure 3 (first and second columns, respectively). The general model reproduced mean observed variables satisfactorily for both the parameterization and test sites; however, all r^2 values in both cases were 0 or close to 0 (means, r^2 values and root-means-square errors are reported in Figure 3). There were positive correlations between observations and modeled values for soil C, N, and P, the soil C:N ratio, and DON, although none were significant. There were no correlations between the observed and modeled DOC and dissolved inorganic N fluxes. For the test data set, correlations between observed and modeled soil C, N, and P were weakened, but the correlations for inorganic N leaching and soil C:N ratio were strengthened and were significant ($p < 0.05$ and $p < 0.005$, respectively). Root-mean-square errors (RMSE) between observations and predictions did not systematically decrease between parameterization and test sites. Overall, there was no consistent degradation in model performance between parameterization and testing.

Figure 3 (right column) shows that model performance across soil nutrient pools was markedly improved by allowing P_{weath0} to vary on a site-by-site basis, as described in section 2.4. Correlations between modeled and observed outputs were increased, and all were significant ($p < 0.001$). The intercepts of these correlations were also reduced bringing the results closer to the one-to-one line. Positive r^2 values were produced for the C, N, and P soil pools by the P_{weath0} site calibrated results, and RMSE values were reduced.

The resultant site-specific P_{weath0} values were log-normally distributed between 50 and 720 g m^{-2} with a geometric mean of 145 g m^{-2} (Figure S5). As expected, a strong ($r^2 = 0.60$, $p < 0.001$) positive correlation is found between site-specific P_{weath0} and measured P_{SOM}. The mean site-specific P_{weath0} value for podzols and rankers is lower than the mean for other soils, by a factor of 1.2, in line with the observed difference in topsoil P_{SOM} between these soil groups. However, the difference was not significant ($p > 0.25$). No relationship of site-specific P_{weath0} with pH ($r^2 = 0.03$, $p > 0.1$) was found, nor with PFT, nor geographical location (Figure S5).

3.2. Time Series Results

Using generalized parameter set, we examined general temporal trends in system C, N, and P using four generic sites (one for each PFT), driven by median climate and deposition forcings. The soil type was set to podzolic for each of the four sites. Figures 4–6 give results for these generic sites.

The calculated initial accumulation rates of C, N, and P are such that the C pool took approximately 4000 years to reach 1000 g m^{-2} (Figure 4), which is appreciably slower than found in most chronosequence or recolonization studies [*Anderson*, 1977; *Jones et al.*, 2008; *Mavris et al.*, 2010; *Phillips et al.*, 2008; *Richardson et al.*, 2004]. This may reflect underestimation of the N fixation rate under early conditions, because our modeling of N fixation, dependent only upon P availability and temperature (equation (11)), is too simple, for example, neglecting early colonization by N-fixers [*S K Schmidt et al.*, 2008]. However, contemporary early soil formation may be influenced by neighboring [*Anderson*, 1977], N deposition [*Jones et al.*, 2008], and higher temperatures and therefore not be directly comparable to conditions following deglaciation. Nonetheless, the C, N, and P pools subsequently build up to reach realistic levels by 5000 B.P. (i.e., 3000 B.C.), after which they change only slowly, although true steady states are not attained.

Between 1800 and 2000, the increasing influence of anthropogenic atmospheric N deposition caused 1.9 to 3.3-fold increases in NPP attributable to elevated N deposition (Figure 4). Likewise, topsoil C pools increase

1.25 to 2 times, and topsoil N pools increase 1.2–1.8 times over this period. Topsoil P declines, however, as elevated N deposition alleviates N limitation of NPP, and increasing quantities of P are acquired from the SOM to support this growth. Also, larger pools of C and N in the soil lead to greater production of DOM, given the constant turnover rates. As such, there is also a contemporary rise in P loss via DOP.

Comparing the PFTs, the N14CP model shows marked differences in SON between tree and nontree plant types, with lower soil N under trees. This is attributable to the larger biomass pools of N and P in the tree PFTs within the model. The difference between tree and nontree PFTs is also borne out in the field data, with topsoil organic N pools being significantly higher in shrub and herbaceous sites than broadleaf and deciduous sites ($p < 0.001$), with means of 438 g-N m^{-2} and 316 g-N m^{-2}, respectively. The modeled broadleaf site (Figure 4) shows the strongest response to the elevated N deposition, as this site receives the most deposition (the PFT N deposition median is highest for broadleaf sites) and subsequently has the biggest increase in plant available N (Figure 4). The response in topsoil N:P in broadleaf ecosystems is particularly marked, as an amplifying effect is seen as topsoil is enriched by deposition and P in the SOM is reduced as plants start to acquire P from this source for growth to stoichiometrically match the increasing N.

Comparing the results in Figure 4 to those of the C-N model of N14C [*Tipping et al.*, 2012a, 2012b], generally, the effects of N deposition on NPP and soil pools are of similar magnitudes.

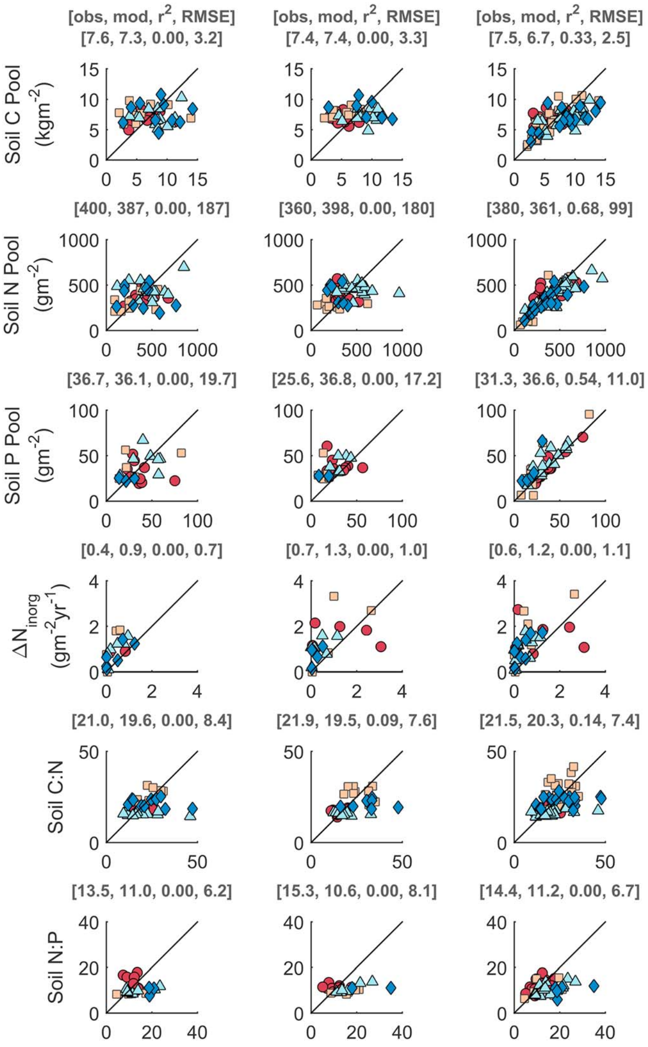

Figure 3. Observations (*x* axis) versus N14CP model simulations (*y* axis). (left column) Observations and model outputs for parameterization sites using the generalized parameter set. (middle column) Observations and model outputs for test sites using the generalized parameter set. (right column) Observations and model outputs for all sites in the data set when the initial pool of weatherable P is allowed to vary on a site-by-site basis, and the value of P_{weath0} is chosen by minimizing the site observation-mode residuals. Contemporary plant cover is denoted by marker style: broadleaf forest is denoted by a circle, coniferous forest by a square, shrubland by a diamond, and herbaceous plant cover by a triangle. Lines are the one-to-one relationship between observation and model. The mean of the observations and the model and the r^2 and root-mean-square errors (RMSE) are given in the titles.

The premodern N fixation rate assumed in N14C based on literature values falls within the upper end of the range of N fixation rates simulated in N14CP. A rate of 0.3 g m^{-2} was used in N14C, and the rate in N14CP is 0.17–0.21 g m^{-2} (Figure 4) and 0.27–0.35 g m^{-2} for podzol/rankers and nonpodzol/rankers, respectively, as determined by the parameterization.

3.2.1. Phosphorus Dynamics

At the start of the simulation all the P is in weatherable rock (Figure 5), and this source diminishes owing to leaching losses of P_{inorg} and DOP over time, so that the present total P pool is about 50% of the initial one. The temporal changes in soil P pools are in line with the findings of *TW Walker and Syers* [1976] and *Buendía et al.* [2010]. Initially, weathered P is mainly transferred to the sorbed pool, then the organic pool develops along

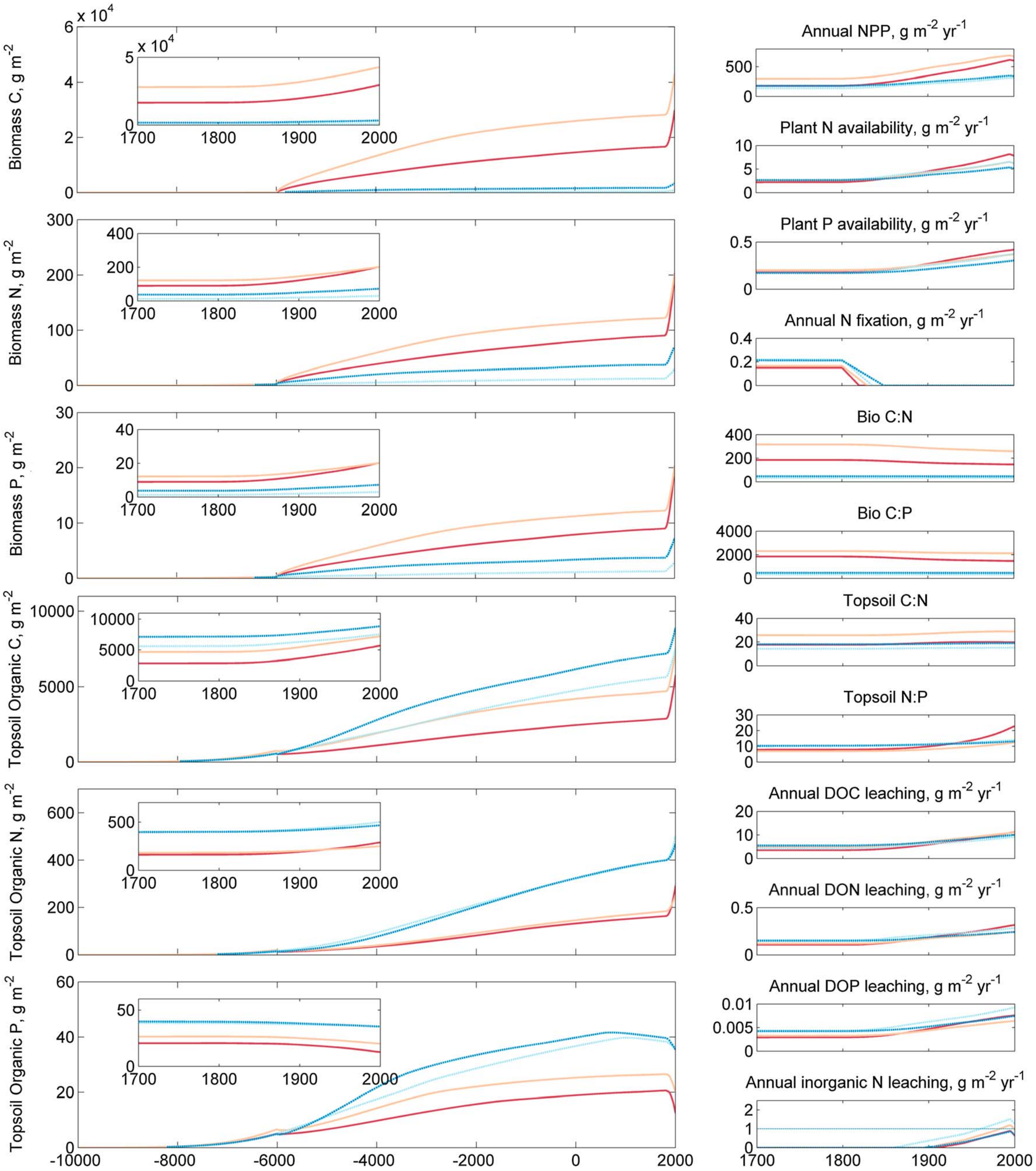

Figure 4. Time series results using the generalized parameter set for four sites with varying plant functional type (broadleaf: red line, conifer: yellow line, herbaceous: light blue, shrub: dark blue line), driven with median climate and deposition conditions. All sites start with herbaceous vegetation and transition to their modern day vegetation type in 6000 B.C. (broadly concurring with estimates of northern Europe succession dates postglaciation).

with the biomass and soil N pools. The vegetation then diverts P from sorbing to soil surfaces, and by modern times the majority of P is stored within the SOP, as is observed for young temperate soils. However, as N availability increases with modern day N deposition, more available P is taken up in growth increasing the total P held within the vegetation pools. As plants can access P in SOP within the model if there is sufficient N, then there is a reduction in SOP. It is also evident in these plots that, over long timescales, the rate of loss in P is declining. Dissolved inorganic leaching fluxes of P peak and decline in line with the soil inorganic P pool (Figure 6). The DOP initially increases with SOP. However, between 4000 and 2000 B.C. the vegetation starts accessing the DOP for growth, creating a decline in the DOP leaching rate from 4000 B.C. to 1800 A.D.

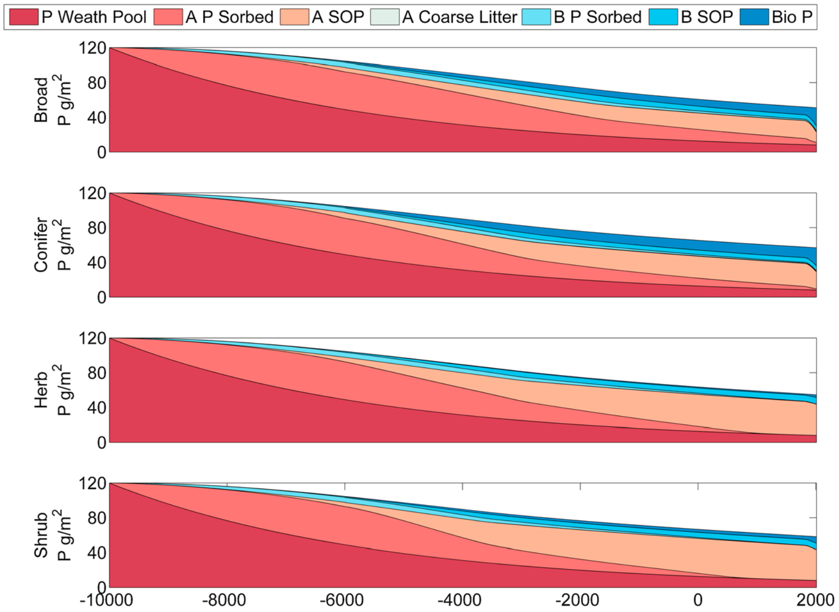

Figure 5. Changes in modeled P stores between 10,000 B.C., which marks the recession of the ice and commencement of weathering, to 2000 A.D. As for Figure 4, the model was driven with median climate and deposition conditions.

If a nonpodzol/ranker soil is assumed, then the initial pool of weatherable P is larger, resulting in larger topsoil organic C, N, and P pools in the order of 10–20% for C, 20–50% for N, and 65–140% for soil P. These larger pool sizes are attributable to long-term changes in N fixation rather than increased P availability in the short term, i.e., contemporary NPP is not significantly increased (0.1–3%). This indicates that the sensitivity of contemporary soil C, N, and P pools to the P weathering source results from the links made between N fixation and P availability.

4. Discussion

4.1. Weatherable P as a Control on Soil C, N, and P

Fundamental to the development of these ecosystems is the weathering input of P, which not only acts as a plant nutrient but also affects biomass and carbon accumulation through its influence on N fixation. The results from site-specific variation of P_{weath0} (Figure 3, right column) demonstrate its strong effects on predicted contemporary soil C, N, and P pools. When P_{weath0} is allowed to vary within sensible ranges for rock P content and P weathering fluxes, the improvements in the prediction of soil C and N, as well as soil P, are striking. This dynamic ecosystem modeling has quantitatively produced behaviors that agree with the deductions made on the basis of soil C, N, and P concentrations by Walker and colleagues [*T. Walker and Adams*, 1958; *TW Walker and Syers*, 1976] regarding the key influence of P on the biogeochemical cycles of C and N and on soil fertility.

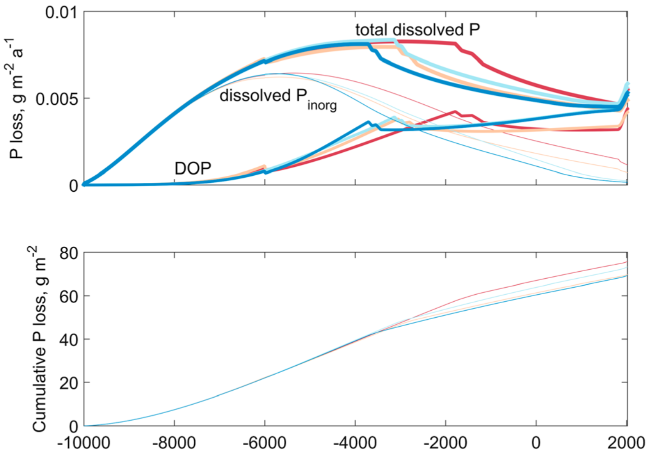

Figure 6. Leaching losses of P, modeled with median climate and deposition conditions. (top) inorganic, organic, and total fluxes for different PFT (broadleaf: red line, conifer: yellow line, herbaceous: light blue, shrub: dark blue line). (bottom) Cumulative losses.

In making comparisons of our estimates of P_{weath0} and P weathering rates with lithologically based data [*Hartmann and Moosdorf*, 2011, 2012; *Hartmann* *et al.*, 2012, 2014; *Xiaojuan Yang et al.*, 2013], it needs to be borne in mind that because our model involves the dissolution of a specified amount of apatite, the weatherable pools and fluxes change over time, as in the conceptual model of *TW Walker and Syers* [1976]. Thus, our analysis produces an average contemporary P weathering rate of about 0.003 $\mathrm{g\,m^{-2}\,a^{-1}}$, while the initial rate was about 10 times higher. A different approach to the estimation of P weathering inputs is from the approach of *Hartmann and Moosdorf* [2012] who estimated them by combining the hydrochemical flux of Si (assumed not to be significantly affected soil processes) with P/Si rock ratios. From the mapped global lithological map (GLiM) lithology [*Hartmann and Moosdorf*, 2012] and P weathering data by rock type [*Hartmann et al.*, 2014], an average weathering input of P at our field sites of about 0.012 $\mathrm{g\,m^{-2}\,a^{-1}}$ is obtained. This is bracketed by our initial and contemporary fluxes, and the independent approaches (modeling and hydrogeology) yield order-of-magnitude agreement.

However, the site-specific model-derived weathering rates do not correlate with the lithologically based values ($r^2 = 0.0$, $p > 0.7$, $n = 84$), which precludes the use of the latter in our modeling. The lack of correlation is perhaps not surprising given that the lithological mapping, although high resolution in global terms, is coarse at the scales of our sites. The average GLiM polygon has an area of approximately 400 $\mathrm{km^2}$, providing considerable scope for lithological and P source heterogeneity. The higher resolution of soil mapping, and the tendency of soil type to reflect parent mineral properties, probably explains the modest predictive power obtained by putting the sites into two classes (podzols/rankers and other soils), but we note that the significant difference between the two classes does not apply for the site-specific P_{weath0} values. Neither did we find any significant variation of P_{weath0} with geographical location, PFT, or pH. Thus, currently available data sets offer little possibility of predicting P weathering or P_{weath0} and associated spatial variability in soil C and N pools and ecosystem productivity. Predictive modeling is therefore restricted to average conditions over many sites, as in Figure 3. Systematic research is required to characterize field sites on soils with selected parent materials varying in P content and then combine the results with dynamic modeling using N14CP and other models.

4.2. Nutrient Limitations to Plant Productivity

In the model, NPP at all 88 sites was nutrient limited, rather than temperature or precipitation limited. The sites were predominantly N limited. Only one site was P limited for results using the general P_{weath0} values, rising to 15 P limited sites when using the site-specific P_{weath0}. Of the P-limited sites for the latter, there was no dominance of vegetation type or geographical location; however, the soils were predominantly podzolic (11 out of 15). Interestingly, the mean N deposition to the P limited sites was significantly higher than that to the non-P-limited sites ($p < 0.05$), and the observed N pools were also found to be significantly lower ($p < 0.001$). This suggests that the site-specific calibration of P_{weath0} has attributed low P availability to sites where observation of soil N are low given the level of N deposition, thus limiting development of soil N. This may actually be the case, or it is possible that the N deposition estimate for these sites is too high, or soil observation of N is uncharacteristically low. It is also possible that the model has not sufficiently captured the cause of difference between sites. Only three of the P-limited sites have soil organic P observations, so it is difficult to determine whether the model is falsely predicting low P in these cases. However, for the three observations that were available, one site has lower modeled topsoil organic P (by 60%), and the other two have higher modeled topsoil organic P (by 17% and 48%), indicating that the model is not consistently underestimating P to account for a lack of N.

In N14CP, plant uptake of inorganic N and P is prioritized over their immobilization into SOM, and as a result, for the N-limited systems that make up the great majority of our field sites, all available inorganic N is used for plant growth during the growing season, and (net) immobilization occurs only during the nongrowing season. This allows plant stoichiometric requirements for nutrients to be met and sensible values of NPP to be achieved, while the SOM can sequester N in the long term. Plainly, nutrient immobilization by microbes must actually occur during the growing season, but the implication is that recycling results in no net immobilization. As explained by *Kaye and Hart* [1997] this situation can arise because "even if plants/mycorrhizae are relatively unsuccessful competitors for N during individual competition events, they can accumulate N for growth by competing several times for the same N atom and then storing N in plant tissues". Thus, at the quarterly time step employed in N14CP, the simplifying assumption that plants have priority for nutrients during the growing season can be justified, and we assume it applies to both N and P. Consequential simulation outcomes are (1) zero inorganic N leaching rates from topsoil during the growing season and (2) the removal (partial to nearly complete) of atmospherically deposited N by the ecosystem. These predictions are in broad agreement with observed surface water NO_3-N fluxes in UK upland areas receiving high atmospheric N deposition; the fluxes are low in summer but relatively high in winter, although lower than atmospheric inputs [*Neal et al.*, 2003; *Tipping et al.*, 2012a, 2012b].

Our approach to modeling ecosystem development relies on the strong empirical evidence that productivity of temperate natural and seminatural ecosystems is limited by N and sometimes P [*Elser et al.*, 2007; *Vitousek et al.*, 2010]. In N14CP, if neither of these nutrients is limiting, NPP is determined by either temperature or precipitation. We neglect possible CO_2 fertilization, which may be significant given that the atmospheric CO_2 concentration has risen by approximately 40% since 1800 and is projected to be more than twice the 1800 value by the end of the 21st century [*International Panel on Climate Change* (*IPCC)*, 2014]. Some free-air CO_2 enrichment experiments show an increase in forest NPP in response to a step change of 200 ppmv in atmospheric CO_2 concentration, for example, at the N-limited Duke University site an enhancement in NPP of approximately 30% is reported [*McCarthy et al.*, 2010]. According to *Drake et al.* [2011] this could arise by the stimulation of soil microbial activity under elevated CO_2 causing a faster turnover of SOM and acceleration of N cycling. Such an effect might be incorporated into N14CP, via an empirical relationship between CO_2 concentration and SOM turnover rate constants. However, *Drake et al.* [2011] also pointed out that observed ecosystem responses to experimentally elevated atmospheric CO_2 concentration vary widely, from no response to transient and sustained increases in NPP. Furthermore, an assessment of the outputs of seven forest models (appreciably more detailed than N14CP with respect to plant physiology and soil biogeochemistry) concluded that there are significant uncertainties especially in the N cycle that hamper prediction of CO_2 effects [*A P Walker et al.*, 2015]. Therefore, it is premature to include a representation of CO_2 effects in N14CP. It can also be noted that modeled increases in NPP over 300 years as a result of a step change in CO_2 concentration from 380 to 550 ppmv are typically 20% [*A P Walker et al.*, 2015], which is modest in comparison to the 200 to 300% increases simulated in response to N deposition in northern Europe (Figure 4).

4.3. Atmospheric N Deposition and P

Increased atmospheric N deposition was shown to have a large effect on NPP and soil C and N pools in the model (Figure 4), which is understandable given that the sites were most commonly N limited. The calculated increase in tree biomass C over the period 1800–2000 (Figure 4) corresponds to an increase of 60 gC/g atmospherically deposited N, or 30 $gC\,gN^{-1}$ if only aboveground biomass is considered. This is about 50% of the value of 61 $gC\,gN^{-1}$ estimated by *Quinn Thomas et al.* [2010] from US forestry inventory data but is in the middle of the range of 15–40 $gC\,gN^{-1}$ estimated for European forests by *de Vries et al.* [2009]. Therefore, our calculated effects are quantitatively realistic, at least in terms of tree NPP and biomass.

The magnitudes of increases in NPP, soil C, and N agree with previous results from N14C, which did not incorporate P cycling [*Tipping et al.*, 2012a, 2012b], suggesting that while P is important in long-term soil C and N development, P has not suppressed the response to N deposition at these sites. By integrating the cycles of C, N, and P, we can also examine the influence of C and N on P. The model indicates that increases in N and C caused by atmospheric N deposition may accelerate P loss in ecosystems by DOP leaching. Increased turnover of newly sequestered C under elevated N levels will lead to a running down of P within the soil as P is not renewed from exogenous sources, assuming decomposition of C, N, and P is under stoichiometric control, as is the case in N14CP.

4.4. No Significant pH Effect on Decomposition and Immobilization

The modeling revealed only a small dependence of SOM turnover or nutrient immobilization on pH. This is contrary to the prevailing opinion that the rates of these processes are significantly lower under acid conditions [*Leifeld et al.*, 2013; *Walse et al.*, 1998]. Evidently, although the present data covered a range of soil pH (Figure 2), factors other than pH had more influence on the model parameterization. It may be that the model would find a pH dependence if the spatial data employed here were supplemented with time series data, for example, the observations of *Oulehle et al.* [2011] that in the Czech Republic forest floor organic matter declined as a result of acidification reversal over the period 1995–2009.

4.5. Extension to Other Ecosystem Types

The N14CP model in its current version simulates macronutrient behavior in temperate ecosystems with young soils, with a sufficiently simple process representation to permit parameterization from field data. This is already useful in the analysis and potential prediction of C, N, and P cycling in systems such as those of northern Europe that are experiencing high N deposition. To make the model more globally applicable, i.e., extending the approach to a wider range of ecosystems, additional factors would need to be considered. Given the importance of P availability in ecosystem development, then over geological timescales (circa 10^6 years) a significant issue is the replenishment of weatherable P by tectonic uplift, as emphasized in the global P modeling of *Buendía et al.* [2010], which would need to be added to the model to simulate ecosystems on older soils. The wider variations water availability at global scales would need to be factored in with respect to both weathering and element losses by leaching, secondary mineral formation, and temperature effects on weathering [cf. *Goll et al.*, 2014] might need to be included. Element losses by physical erosion would be more important in some ecosystems. The simulation of agricultural systems would need to account for biomass removal in cropping and the effects of intensive grazing. The simulation of peatlands would require a version of the model able to deal with the burial of carbon in the anoxic catotelm and recognizing the importance to such systems of P inputs by atmospheric deposition and biological transfers [*Tipping et al.*, 2010]. Basic field data comprising soil variables, including radiocarbon data, and NPP for parameterization and testing could be applied at the global scale in a similar way to that adopted here. In addition, chronosequence data [e.g., *Richardson et al.*, 2004] could be used. Working at the larger scale would likely produce more insights through the more effective use of lithological data (section 4.1) to predict weathering rates, not only of P but also base cations, and mineral N present in sedimentary rocks [*Morford et al.*, 2011].

5. Conclusions

A new model, N14CP, integrating terrestrial carbon, nitrogen, and phosphorus cycles that is suitable for long-term application (~10,000 years) in temperate/boreal Northern Hemisphere ecosystems at regional scales has been presented. The model addresses an important requirement for models that are applicable at scales above the site scale but constrainable against observation data. The model has been parameterized and tested using field observations from 88 sites in northern Europe across broadleaf, conifer, shrub, and herbaceous habitats, making it the most robustly tested model of C, N, and P cycles to date. With available driving data (climate, vegetation history, and N deposition), it has been demonstrated that the model can represent broad contemporary trends in nutrient change across multiple soil nutrient pools and fluxes. However, smaller intersite variation was not well reproduced.

The study highlighted the importance of weatherable P as a control on the long-term development of ecosystem C, N, and P. This mainly arises because of the assumed dependence of N fixation, and consequent C fixation, on P availability. Model performance across C, N, and P variables was considerably improved when the initial weatherable P was allowed to vary site-by-site within boundaries reasonable for the variation in lithology. This yielded a range of 50 to 720 g m^{-2} of weatherable P and resulted in appreciable increases in goodness of fit. However, we could not find a predictive variable in soil type, lithology or pH, etc. for this variation. Finer-scale spatial characterization of weatherable P is needed to determine if intersite variation can be explained by this variable. Alternatively, a study analyzing model performance at regional scales against observations across systematically chosen lithological types would help determine whether available lithological data are informative for this purpose at larger scales.

All sites were found to be nutrient limited in the simulations and most commonly N limited. As such, the model predicted that elevated N deposition since 1800 has considerably increased soil C and N and net primary productivity, under median conditions doubling or tripling NPP, leading to higher plant biomass. The increase in biomass C per N deposition ratio of 30 for median conditions is in line with literature data. The effects of N deposition have not been suppressed by a lack of P, at least for the relatively young soils (~12,000 years) of the sites examined.

Acknowledgments
We thank M. Vieno (Centre for Ecology and Hydrology) and B. Rihm (METEOTEST, Switzerland) for the provision of deposition data, C.L. Bryant (NERC Radiocarbon Facility) for advice on radiocarbon, A.F. Harrison (Centre for Ecology and Hydrology) for the provision of soils data, and R. Tipping for help with data collation. We are also grateful to the Editor (S.Trumbore) and three referees for their constructive comments. All data can be requested from the corresponding author (Jessica Davies, j.davies4@lancaster.ac.uk). This research was funded by the UK Natural Environment Research Council Macronutrient Cycles Programme (LTLS project, grant NE/J011533/1 NE/J011703/1 and NE/J011630/1) and the Scottish Government.

References

Anderson, D. W. (1977), Early stages of soil formation on glacial till mine spoils in a semi-arid climate, *Geoderma*, *19*(1), 11–19.

Andersson, P., D. Berggren, and I. Nilsson (2002), Indices for nitrogen status and nitrate leaching from Norway spruce (Picea abies (L.) Karst.) stands in Sweden, *For. Ecol. Manage.*, *157*(1), 39–53.

Beier, C., B. A. Emmett, A. Tietema, I. K. Schmidt, J. Peñuelas, E. K. Láng, P. Duce, P. De Angelis, A. Gorissen, and M. Estiarte (2009), Carbon and nitrogen balances for six shrublands across Europe, *Global Biogeochem. Cycles*, *23*, GB4008, doi:10.1029/2008GB003381.

Berggren, D., B. Bergkvist, M.-B. Johansson, P.-A. Melkerud, A. Nilsson, M. Olsson, O. Langvall, H. Majdi, and P. Weslien (2004), A description of LUSTRA's common field sites *Rep.*, Swedish Univ. of Agricultural Sciences, Uppsala (Sweden). Dept. of Forest Soils.

Berner, R. A. (1992), Weathering, plants, and the long-term carbon cycle, *Geochim. Cosmochim. Acta*, *56*(8), 3225–3231.

Blaser, P., S. Zimmermann, J. Luster, L. Walthert, and P. Lüscher (2005), *Waldböden der Schweiz. Band 2. Region Alpen und Alpensüdseite. Birmensdorf, WSL*, Hep Verlag, Bern.

Bloemerts, M., and W. D. Vries (2009), Relationships between nitrous oxide emissions from natural ecosystems end environmental factors.

Bol, R. A., D. D. Harkness, Y. Huang, and D. M. Howard (1999), The influence of soil processes on carbon isotope distribution and turnover in the British uplands, *Eur. J. Soil Sci.*, *50*(1), 41–51.

Boyle, J. F., R. C. Chiverrell, S. A. Norton, and A. J. Plater (2013), A leaky model of long-term soil phosphorus dynamics, *Global Biogeochem. Cycles*, *27*, 516–525, doi:10.1002/gbc.20054.

Brady, P. V., and S. A. Carroll (1994), Direct effects of CO_2 and temperature on silicate weathering: Possible implications for climate control, *Geochim. Cosmochim. Acta*, *58*(7), 1853–1856.

Buendía, C., A. Kleidon, and A. Porporato (2010), The role of tectonic uplift, climate, and vegetation in the long-term terrestrial phosphorous cycle, *Biogeosciences*, *7*(6), 2025–2038.

Campolongo, F., J. Cariboni, and A. Saltelli (2007), An effective screening design for sensitivity analysis of large models, *Environ. Modell. Software*, *22*(10), 1509–1518.

Cleveland, C. C., A. R. Townsend, D. S. Schimel, H. Fisher, R. W. Howarth, L. O. Hedin, S. S. Perakis, E. F. Latty, J. C. Von Fischer, and A. Elseroad (1999), Global patterns of terrestrial biological nitrogen (N_2) fixation in natural ecosystems, *Global Biogeochem. Cycles*, *13*(2), 623–645.

Corre, M. D., and N. P. Lamersdorf (2004), Reversal of nitrogen saturation after long-term deposition reduction: Impact on soil nitrogen cycling, *Ecology*, *85*(11), 3090–3104.

Crews, T. E., H. Farrington, and P. M. Vitousek (2000), Changes in asymbiotic, heterotrophic nitrogen fixation on leaf litter of Metrosideros polymorpha with long-term ecosystem development in Hawaii, *Ecosystems*, *3*(4), 386–395.

Danger, M., T. Daufresne, F. Lucas, S. Pissard, and G. Lacroix (2008), Does Liebig's law of the minimum scale up from species to communities?, *Oikos*, *117*(11), 1741–1751.

Davis, B. A. S., S. Brewer, A. C. Stevenson, and J. Guiot (2003), The temperature of Europe during the Holocene reconstructed from pollen data, *Quat. Sci. Rev.*, *22*(15–17), 1701–1716.

de Vries, W., G. Schütze, S. Lofts, E. Tipping, M. Meili, P. Römkens, and J. Groenenberg (2005), Calculation of critical loads for cadmium, lead and mercury; background document to a mapping manual on critical loads of cadmium, lead and mercury *Rep.*, Alterra.

de Vries, W., S. Solberg, M. Dobbertin, H. Sterba, D. Laubhann, M. Van Oijen, C. Evans, P. Gundersen, J. Kros, and G. Wamelink (2009), The impact of nitrogen deposition on carbon sequestration by European forests and heathlands, *For. Ecol. Manage.*, *258*(8), 1814–1823.

DEFRA (2006), *UKAWMN Summary of Data for Year 18 (2005-2006)*, edited by E. M. Shilland et al., London.

Drake, J. E., A. Gallet-Budynek, K. S. Hofmockel, E. S. Bernhardt, S. A. Billings, R. B. Jackson, K. S. Johnsen, J. Lichter, H. R. McCarthy, and M. L. McCormack (2011), Increases in the flux of carbon belowground stimulate nitrogen uptake and sustain the long-term enhancement of forest productivity under elevated CO_2, *Ecol. Lett.*, *14*(4), 349–357.

Eisele, L., D. Schimel, L. Kapustka, and W. Parton (1989), Effects of available P and N: P ratios on non-symbiotic dinitrogen fixation in tallgrass prairie soils, *Oecologia*, *79*(4), 471–474.

Elser, J. J., M. E. S. Bracken, E. E. Cleland, D. S. Gruner, W. S. Harpole, H. Hillebrand, J. T. Ngai, E. W. Seabloom, J. B. Shurin, and J. E. Smith (2007), Global analysis of nitrogen and phosphorus limitation of primary producers in freshwater, marine and terrestrial ecosystems, *Ecol. Lett.*, *10*(12), 1135–1142.

Emmett, B. A., C. Beier, M. Estiarte, A. Tietema, H. L. Kristensen, D. Williams, J. Penuelas, I. Schmidt, and A. Sowerby (2004), The response of soil processes to climate change: Results from manipulation studies of shrublands across an environmental gradient, *Ecosystems*, *7*(6), 625–637.

Emmett, B., B. Reynolds, P. Chamberlain, E. Rowe, D. Spurgeon, S. Brittain, Z. Frogbrook, S. Hughes, A. Lawlor, and J. Poskitt (2010), Countryside survey: Soils report from 2007.

Evans, C., B. Reynolds, C. Curtis, H. Crook, D. Norris, and S. Brittain (2005), A conceptual model of spatially heterogeneous nitrogen leaching from a Welsh moorland catchment, *Water, Air, & Soil Pollut.: Focus*, *4*(6), 97–105.

Galloway, J. N., F. J. Dentener, D. G. Capone, E. W. Boyer, R. W. Howarth, S. P. Seitzinger, G. P. Asner, C. Cleveland, P. Green, and E. Holland (2004), Nitrogen cycles: Past, present, and future, *Biogeochemistry*, *70*(2), 153–226.

Goll, D., V. Brovkin, B. Parida, C. Reick, J. Kattge, P. Reich, P. Van Bodegom, and Ü. Niinemets (2012), Nutrient limitation reduces land carbon uptake in simulations with a model of combined carbon, nitrogen and phosphorus cycling, *Biogeosci. Discuss.*, *9*(3), 3173–3232.

Goll, D., N. Moosdorf, J. Hartmann, and V. Brovkin (2014), Climate-driven changes in chemical weathering and associated phosphorus release since 1850: Implications for the land carbon balance, *Geophys. Res. Lett.*, *41*, 3553–3558, doi:10.1002/2014GL059471.

Gundersen, P. (1995), Nitrogen deposition and leaching in European forests—Preliminary results from a data compilation, *Water Air Soil Pollut.*, *85*(3), 1179–1184.

Hartmann, J., and N. Moosdorf (2011), Chemical weathering rates of silicate-dominated lithological classes and associated liberation rates of phosphorus on the Japanese Archipelago—Implications for global scale analysis, *Chem. Geol.*, *287*(3–4), 125–157.

Hartmann, J., and N. Moosdorf (2012), The new global lithological map database GLiM: A representation of rock properties at the Earth surface, *Geochem. Geophys. Geosyst.*, *13*, Q12004, doi:10.1029/2012GC004370.

Hartmann, J., H. Dürr, N. Moosdorf, M. Meybeck, and S. Kempe (2012), The geochemical composition of the terrestrial surface (without soils) and comparison with the upper continental crust, *Int. J. Earth Sci. (Geol Rundsch)*, *101*(1), 365–376.

Hartmann, J., N. Moosdorf, R. Lauerwald, M. Hinderer, and A. J. West (2014), Global chemical weathering and associated P-release—The role of lithology, temperature and soil properties, *Chem. Geol.*, *363*, 145–163.

International Panel on Climate Change (2014), Carbon Dioxide. [Available at: http://www.ipcc-data.org/observ/ddc_co2.html, accessed 11 February 2015.]

Jackson-Blake, L., R. Helliwell, A. Britton, S. Gibbs, M. Coull, and L. Dawson (2012), Controls on soil solution nitrogen along an altitudinal gradient in the Scottish uplands, *Sci. Total Environ.*, *431*, 100–108.

Jones, M. L. M., A. Sowerby, D. L. Williams, and R. E. Jones (2008), Factors controlling soil development in sand dunes: Evidence from a coastal dune soil chronosequence, *Plant Soil*, *307*(1–2), 219–234.

Kaiser, K., and K. Kalbitz (2012), Cycling downwards—Dissolved organic matter in soils, *Soil Biol. Biochem.*, *52*, 29–32.

Kaiser, K., G. Guggenberger, and L. Haumaier (2003), Organic phosphorus in soil water under a European beech (Fagus sylvatica L.) stand in northeastern Bavaria, Germany: Seasonal variability and changes with soil depth, *Biogeochemistry*, *66*(3), 287–310.

Kaye, J. P., and S. C. Hart (1997), Competition for nitrogen between plants and soil microorganisms, *Trends Ecol. Evol.*, *12*(4), 139–143.

Kleja, D. B., M. Svensson, H. Majdi, P.-E. Jansson, O. Langvall, B. Bergkvist, M.-B. Johansson, P. Weslien, L. Truusb, and A. Lindroth (2008), Pools and fluxes of carbon in three Norway spruce ecosystems along a climatic gradient in Sweden, *Biogeochemistry*, *89*(1), 7–25.

Knoll, M. A., and W. C. James (1987), Effect of the advent and diversification of vascular land plants on mineral weathering through geologic time, *Geology*, *15*(12), 1099–1102.

Kreutzer, K., C. Beier, M. Bredemeier, K. Blanck, T. Cummins, E. Farrell, N. Lammersdorf, L. Rasmussen, A. Rothe, and P. De Visser (1998), Atmospheric deposition and soil acidification in five coniferous forest ecosystems: A comparison of the control plots of the EXMAN sites, *For. Ecol. Manage.*, *101*(1), 125–142.

Lamersdorf, N. P., and M. Meyer (1993), Nutrient cycling and acidification of a northwest German forest site with high atmospheric nitrogen deposition, *For. Ecol. Manage.*, *62*(1–4), 323–354.

Leifeld, J., S. Bassin, F. Conen, I. Hajdas, M. Egli, and J. Fuhrer (2013), Control of soil pH on turnover of belowground organic matter in subalpine grassland, *Biogeochemistry*, *112*(1–3), 59–69.

Lottig, N. R., E. H. Stanley, and J. T. Maxted (2012), Assessing the influence of upstream drainage lakes on fluvial organic carbon in a wetland-rich region, *J. Geophys. Res.*, *117*, G03011, doi:10.1029/2012JG001983.

MacDonald, J., N. Dise, E. Matzner, M. Armbruster, P. Gundersen, and M. Forsius (2002), Nitrogen input together with ecosystem nitrogen enrichment predict nitrate leaching from European forests, *Global Change Biol.*, *8*(10), 1028–1033.

Mackenzie, F. T., L. M. Ver, and A. Lerman (2002), Century-scale nitrogen and phosphorus controls of the carbon cycle, *Chem. Geol.*, *190*(1), 13–32.

Mahowald, N., et al. (2008), Global distribution of atmospheric phosphorus sources, concentrations and deposition rates, and anthropogenic impacts, *Global Biogeochem. Cycles*, *22*, GB4026, doi:10.1029/2008GB003240.

Majer, V., B. J. Cosby, J. Kopácek, and J. Veselý (2003), Modelling reversibility of Central European mountain lakes from acidification: Part I—The Bohemian forest, *Hydrol. Earth Syst. Sci.*, *7*(4), 494–509.

Manzoni, S., and A. Porporato (2009), Soil carbon and nitrogen mineralization: Theory and models across scales, *Soil Biol. Biochem.*, *41*(7), 1355–1379.

Mavris, C., M. Egli, M. Plötze, J. D. Blum, A. Mirabella, D. Giaccai, and W. Haeberli (2010), Initial stages of weathering and soil formation in the Morteratsch proglacial area (Upper Engadine, Switzerland), *Geoderma*, *155*(3), 359–371.

McCarthy, H. R., R. Oren, K. H. Johnsen, A. Gallet-Budynek, S. G. Pritchard, C. W. Cook, S. L. LaDeau, R. B. Jackson, and A. C. Finzi (2010), Re-assessment of plant carbon dynamics at the Duke free-air CO_2 enrichment site: Interactions of atmospheric [CO_2] with nitrogen and water availability over stand development, *New Phytol.*, *185*(2), 514–528.

McGill, W., and C. Cole (1981), Comparative aspects of cycling of organic C, N, S and P through soil organic matter, *Geoderma*, *26*(4), 267–286.

McGroddy, M. E., W. T. Baisden, and L. O. Hedin (2008), Stoichiometry of hydrological C, N, and P losses across climate and geology: An environmental matrix approach across New Zealand primary forests, *Global Biogeochem. Cycles*, *22*, GB1026, doi:10.1029/2007GB003005.

Mills, R. T. E., E. Tipping, C. L. Bryant, and B. A. Emmett (2014), Long-term organic carbon turnover rates in natural and semi-natural topsoils, *Biogeochemistry*, *118*(1–3), 257–272.

Mol-Dijkstra, J., and H. Kros (1999), Modelling effects of acid deposition and climate change on soil and run-off chemistry at Risdalsheia, Norway, *Hydrol. Earth Syst. Sci.*, *5*(3), 487–498.

Morford, S. L., B. Z. Houlton, and R. A. Dahlgren (2011), Increased forest ecosystem carbon and nitrogen storage from nitrogen rich bedrock, *Nature*, *477*(7362), 78–81.

Moulton, K. L., and R. A. Berner (1998), Quantification of the effect of plants on weathering: Studies in Iceland, *Geology*, *26*(10), 895–898.

Moulton, K. L., J. West, and R. A. Berner (2000), Solute flux and mineral mass balance approaches to the quantification of plant effects on silicate weathering, *Am. J. Sci.*, *300*(7), 539–570.

Neal, C., B. Reynolds, M. Neal, L. Hill, H. Wickham, and B. Pugh (2003), Nitrogen in rainfall, cloud water, throughfall, stemflow, stream water and groundwater for the Plynlimon catchments of mid-Wales, *Sci. Total Environ.*, *314–316*, 121–151.

Olander, L. P., and P. M. Vitousek (2000), Regulation of soil phosphatase and chitinase activityby N and P availability, *Biogeochemistry*, *49*(2), 175–191.

Oulehle, F., C. D. Evans, J. Hofmeister, R. Krejci, K. Tahovska, T. Persson, P. Cudlin, and J. Hruska (2011), Major changes in forest carbon and nitrogen cycling caused by declining sulphur deposition, *Global Change Biol.*, *17*(10), 3115–3129.

Parr, T., W. Scott, and A. Lane (1998), The UK environmental change network, in *The International Long Term Ecological Research Network*, pp. 65–73, NERC/Centre for Ecology & Hydrology, Swindon, U. K.

Parton, W. (1996), The CENTURY model, in *Evaluation of Soil Organic Matter Models*, edited, pp. 283–291, Springer, Berlin.

Parton, W., J. Neff, and P. M. Vitousek (2005), Modelling phosphorus, carbon and nitrogen dynamics in terrestrial ecosystems, in *Organic Prosphorus in the Environment*, edited by B. L. Turner, E. Frossard, and D. S. Baldwin, pp. 325–327, CABI, Oxford, U. K.

Pennington, W. (1984), Long-term natural acidification of upland sites in Cumbria: Evidence from post-glacial lake sediments, in *Fifty-Second Annual Report for the Year Ended 31st March 1984*, pp. 28–46, Freshwater Biological Association, Ambleside, U. K.

Phillips, J. D., A. V. Turkington, and D. A. Marion (2008), Weathering and vegetation effects in early stages of soil formation, *Catena*, *72*(1), 21–28.

Pilkington, M. G., S. J. Caporn, J. A. Carroll, N. Cresswell, J. A. Lee, B. Reynolds, and B. A. Emmett (2005), Effects of increased deposition of atmospheric nitrogen on an upland moor: Nitrogen budgets and nutrient accumulation, *Environ. Pollut.*, *138*(3), 473–484.

Qualls, R. G., and B. L. Haines (1991), Geochemistry of dissolved organic nutrients in water percolating through a forest ecosystem, *Soil Sci. Soc. Am. J.*, *55*(4), 1112–1123.

Quinn Thomas, R., C. D. Canham, K. C. Weathers, and C. L. Goodale (2010), Increased tree carbon storage in response to nitrogen deposition in the US, *Nat. Geosci.*, *3*(1), 13–17.

Quirk, J., D. J. Beerling, S. A. Banwart, G. Kakonyi, M. E. Romero-Gonzalez, and J. R. Leake (2012), Evolution of trees and mycorrhizal fungi intensifies silicate mineral weathering, *Biol. Lett.*, *8*(6), 1006–1011.

Raich, J., W. Parton, A. Russell, R. Sanford Jr., and P. Vitousek (2000), Analysis of factors regulating ecosystemdevelopment on Mauna Loa using the Century model, *Biogeochemistry*, *51*(2), 161–191.

Richardson, S., D. Peltzer, R. Allen, M. McGlone, and R. Parfitt (2004), Rapid development of phosphorus limitation in temperate rainforest along the Franz Josef soil chronosequence, *Oecologia*, *139*(2), 267–276.

Rowe, E. C., S. M. Smart, V. H. Kennedy, B. A. Emmett, and C. D. Evans (2008), Nitrogen deposition increases the acquisition of phosphorus and potassium by heather Calluna vulgaris, *Environ. Pollut.*, *155*(2), 201–207.

Schmidt, I. K., A. Tietema, D. Williams, P. Gundersen, C. Beier, B. A. Emmett, and M. Estiarte (2004), Soil solution chemistry and element fluxes in three European heathlands and their responses to warming and drought, *Ecosystems*, *7*(6), 638–649.

Schmidt, S. K., et al. (2008), The earliest stages of ecosystem succession in high-elevation (5000 metres above sea level), recently deglaciated soils, *Proc. R. Soc. B*, *275*, 2793–2802.

Schöpp, W., M. Posch, S. Mylona, and M. Johansson (2003), Long-term development of acid deposition (1880? 2030) in sensitive freshwater regions in Europe, *Hydrol. Earth Syst. Sci. Discuss.*, *7*(4), 436–446.

Schumann, U., and H. Huntrieser (2007), The global lightning-induced nitrogen oxides source, *Atmos. Chem. Phys.*, *7*(14), 3823–3907.

Shepon, A., H. Gildor, L. J. Labrador, T. Butler, L. N. Ganzeveld, and M. G. Lawrence (2007), Global reactive nitrogen deposition from lightning NOx, *J. Geophys. Res.*, *112*, D06304, doi:10.1029/2006JD007458.

Sjøeng, A. M. S., Ø. Kaste, K. Tørseth, and J. Mulder (2007), N leaching from small upland headwater catchments in southwestern Norway, *Water Air Soil Pollut.*, *179*(1–4), 323–340.

Speed, J. D., V. Martinsen, A. Mysterud, J. Mulder, Ø. Holand, and G. Austrheim (2014), Long-term increase in aboveground carbon stocks following exclusion of grazers and forest establishment in an alpine ecosystem, *Ecosystems*, *17*(7), 1138–1150.

Speed, J. D. M., V. Martinsen, A. J. Hester, Ø. Holand, J. Mulder, A. Mysterud, and G. Austrheim (2015), Continuous and discontinuous variation in ecosystem carbon stocks with elevation across a treeline ecotone, *Biogeosciences*, *12*(5), 1615–1627.

Sutton, M. A., A. Bleeker, C. Howard, M. Bekunda, B. Grizzetti, W. D. Vries, H. van Grinsven, Y. Abrol, T. Adhya, and G. Billen (2013), *Our Nutrient World: The Challenge to Produce More Food and Energy With Less Pollution*, Centre for Ecology and Hydrology (CEH) and the United Nations Environment Program (UNEP), Edinburgh, Nairobi.

Taylor, L., J. Leake, J. Quirk, K. Hardy, S. Banwart, and D. Beerling (2009), Biological weathering and the long-term carbon cycle: Integrating mycorrhizal evolution and function into the current paradigm, *Geobiology*, *7*(2), 171–191.

Taylor, L. L., S. A. Banwart, P. J. Valdes, J. R. Leake, and D. J. Beerling (2012), Evaluating the effects of terrestrial ecosystems, climate and carbon dioxide on weathering over geological time: A global-scale process-based approach, *Proc. R. Soc. B*, *367*(1588), 565–582.

Tietema, A., W. De Boer, L. Riemer, and J. Verstraten (1992), Nitrate production in nitrogen-saturated acid forest soils: Vertical distribution and characteristics, *Soil Biol. Biochem.*, *24*(3), 235–240.

Tipping, E., S. Thacker, D. Wilson, and J. Hall (2008), Long-term nitrate increases in two oligotrophic lakes, due to the leaching of atmospherically-deposited N from moorland ranker soils, *Environ. Pollut.*, *152*(1), 41–49.

Tipping, E., P. M. Chamberlain, C. L. Bryant, and S. Buckingham (2010), Soil organic matter turnover in British deciduous woodlands, quantified with radiocarbon, *Geoderma*, *155*(1–2), 10–18.

Tipping, E., P. M. Chamberlain, M. Fröberg, P. J. Hanson, and P. M. Jardine (2012a), Simulation of carbon cycling, including dissolved organic carbon transport, in forest soil locally enriched with 14C, *Biogeochemistry*, *108*(1–3), 91–107.

Tipping, E., E. Rowe, C. Evans, R. Mills, B. Emmett, J. Chaplow, and J. Hall (2012b), N14C: A plant–soil nitrogen and carbon cycling model to simulate terrestrial ecosystem responses to atmospheric nitrogen deposition, *Ecol. Modell.*, *247*, 11–26.

Tipping, E., et al. (2014), Atmospheric deposition of phosphorus to land and freshwater, *Environ. Sci.: Processes Impacts*, *16*(7), 1608–1617.

UKREATE (2010), Terrestrial Umbrella: Effects of Eutrophication and Acidification on Terrestrial Ecosystems. CEH Contract Report NEC03425. Defra Contract AQ0802.

van Meeteren, M., A. Tietema, E. Van Loon, and J. Verstraten (2008), Microbial dynamics and litter decomposition under a changed climate in a Dutch heathland, *Appl. Soil Ecol.*, *38*(2), 119–127.

van Veen, J., and E. Paul (1981), Organic carbon dynamics in grassland soils. 1. Background information and computer simulation, *Can. J. Soil Sci.*, *61*(2), 185–201.

van Vuuren, D. P., A. Bouwman, and A. Beusen (2010), Phosphorus demand for the 1970–2100 period: A scenario analysis of resource depletion, *Global Environ. Change*, *20*(3), 428–439.

Ver, L. M. B., F. T. Mackenzie, and A. Lerman (1999), Biogeochemical responses of the carbon cycle to natural and human perturbations: Past, present, and future, *Am. J. Sci.*, *299*(7–9), 762.

Vitousek, P. M., J. D. Aber, R. W. Howarth, G. E. Likens, P. A. Matson, D. W. Schindler, W. H. Schlesinger, and D. G. Tilman (1997), Human alteration of the global nitrogen cycle: Sources and consequences, *Ecol. Appl.*, *7*(3), 737–750.

Vitousek, P. M., S. Porder, B. Z. Houlton, and O. A. Chadwick (2010), Terrestrial phosphorus limitation: mechanisms, implications, and nitrogen-phosphorus interactions, *Ecol. Appl.*, *20*(1), 5–15.

Volk, T. (1987), Feedbacks between weathering and atmospheric CO_2 over the last 100 million years, *Am. J. Sci.*, *287*(8), 763–779.

von Oheimb, G., W. Härdtle, P. S. Naumann, C. Westphal, T. Assmann, and H. Meyer (2008), Long-term effects of historical heathland farming on soil properties of forest ecosystems, *For. Ecol. Manage.*, *255*(5), 1984–1993.

Walker, A. P., et al. (2015), Predicting long-term carbon sequestration in response to CO_2 enrichment: How and why do current ecosystem models differ?, *Global Biogeochem. Cycles*, *29*, 476–495, doi:10.1002/2014GB004995.

Walker, T., and A. F. R. Adams (1958), Studies on soil organic matter: I. Influence of phosphorus content of parent materials on accumulations of carbon, nitrogen, sulfur, and organic phosphorus in grassland soils, *Soil Sci.*, *85*(6), 307–318.

Walker, T., and J. K. Syers (1976), The fate of phosphorus during pedogenesis, *Geoderma*, *15*(1), 1–19.

Walse, C., B. Berg, and H. Sverdrup (1998), Review and synthesis of experimental data on organic matter decomposition with respect to the effect of temperature, moisture, and acidity, *Environ. Rev.*, *6*(1), 25–40.

Walthert, L., S. Zimmermann, P. Blaser, J. Luster, and P. Lüscher (2004), *Waldböden der Schweiz Band 1. Grundlagen und Region Jura (150–163). Birmensdorf, Eidgenössische Forschungsanstalt WSL*, Wiley, Verlag, Weinheim, Germany.

Wang, Y., R. Law, and B. Pak (2010), A global model of carbon, nitrogen and phosphorus cycles for the terrestrial biosphere, *Biogeosciences*, *7*(7), 2261–2282.

Weng, L., F. Vega, and W. Van Riemsdijk (2011), Competitive and synergistic effects in pH dependent phosphate adsorption in soils: LCD modeling, *Environ. Sci. Technol.*, *45*(19), 8420.

White, A. F., A. E. Blum, T. D. Bullen, D. V. Vivit, M. Schulz, and J. Fitzpatrick (1999), The effect of temperature on experimental and natural chemical weathering rates of granitoid rocks, *Geochim. Cosmochim. Acta*, *63*(19), 3277–3291.

Wright, R., C. Beier, and B. Cosby (1998), Effects of nitrogen deposition and climate change on nitrogen runoff at Norwegian boreal forest catchments: The MERLIN model applied to Risdalsheia (RAIN and CLIMEX projects), *Hydrol. Earth Syst. Sci. Discuss.*, *2*(4), 399–414.

Yanai, R. (1992), Phosphorus budget of a 70-year-old northern hardwood forest, *Biogeochemistry*, *17*(1), 1–22.

Yang, X., W. M. Post, P. E. Thornton, and A. Jain (2013), The distribution of soil phosphorus for global biogeochemical modeling, *Biogeosciences*, *10*(4), 2525–2537.

Yang, X., P. Thornton, D. Ricciuto, and W. Post (2014), The role of phosphorus dynamics in tropical forests—A modeling study using CLM-CNP, *Biogeosciences*, *11*(6), 1667–1681.

Zimmermann, S., P. Blaser, J. Luster, L. Waltert, and P. Lüscher (2006), *Waldböden der Schweiz. Band 3. Region Mittelland und Voralpen—Birmensdorf, Eidg. Forschungsanstalt WSL*, vol. 847, Hep Verlag, Bern.